EGFR Juxtamembrane Domain, Membranes, and Calmodulin: Kinetics of Their Interaction

Parijat Sengupta,[†] Eran Bosis,[‡] Esther Nachliel,[‡] Menachem Gutman,[‡] Steven O. Smith,[§] Gyöngyi Mihályné,[†] Irina Zaitseva,[†] and Stuart McLaughlin[†*]

[†]Department of Physiology and Biophysics, Health Sciences Center, Stony Brook University, Stony Brook, New York; [‡]Laser Laboratory for Fast Reactions in Biology, Department of Biochemistry, George S. Wise Faculty of Life Sciences, Tel Aviv University, Tel Aviv, Israel; and [§]Department of Biochemistry and Cell Biology, Center for Structural Biology, Stony Brook University, Stony Brook, New York

ABSTRACT Calcium/calmodulin (Ca/CaM) binds to the intracellular juxtamembrane domain (JMD) of the epidermal growth factor receptor (EGFR). The basic JMD also binds to acidic lipids in the inner leaflet of the plasma membrane, and this interaction may contribute an extra level of autoinhibition to the receptor. Binding of a ligand to the EGFR produces a rapid increase in intracellular calcium, $[Ca^{2+}]_i$, and thus Ca/CaM. How does Ca/CaM compete with the plasma membrane for the JMD? Does Ca/CaM directly pull the JMD off the membrane or does Ca/CaM only bind to the JMD after it has dissociated spontaneously from the bilayer? To answer this question, we studied the effect of Ca/CaM on the rate of dissociation of fluorescent JMD peptides from phospholipid vesicles by making kinetic stop-flow measurements. Ca/CaM increases the rate of dissociation: an analysis of the differential equations that describe the dissociation shows that Ca/CaM must directly pull the basic JMD peptide off the membrane surface. These measurements lead to a detailed atomic-level mechanism for EGFR activation that reconciles the existence of preformed EGFR dimers/oligomers with the Kuriyan allosteric model for activation of the EGFR kinase domains.

INTRODUCTION

The epidermal growth factor receptor (EGFR/ErbB/HER) family of receptor tyrosine kinases has been discussed in many authoritative reviews that highlighted the growing interest in this receptor's mechanism of action in terms of both cell biology and clinical utility (1–6). There is clinical interest because mutations and deletions in the EGFR family are associated with a variety of human cancers, and drugs that interact specifically with these receptors are in clinical use (7–10). Its relevance to cell biology is of interest because the EGFR is the starting point for several different, well-studied cell signaling pathways, such as the calcium/phosphoinositide pathway through the activation of PLC-γ, the PIP_3 pathway through activation of PI3K, and the Ras/MAP-kinase pathway.

Fig. 1 summarizes one current model of EGFR activation adapted from similar figures in the literature (6,11–13). The figure incorporates two recent advances in our understanding of how binding of EGF leads to transautophosphorylation of tyrosine residues in the C-terminal tail of the EGFR, and the subsequent activation of downstream signaling pathways. First, structural studies have revealed that the binding of a ligand to the ''tethered'' extracellular domain of the EGFR produces a conformational change that exposes the dimerization arm (6,13,14). In the conventional paradigm, shown in Fig. 1, the exposed arm allows two EGFR monomers to form a dimer when they diffuse together. This brings the two kinase domains into physical proximity. Second, an elegant report from the Kuriyan laboratory revealed how one kinase domain in a dimer activates its immediate neighbor by an allosteric mechanism (12). Specifically, when the C-terminal or large lobe of one EGFR kinase domain binds to the N-terminal lobe of the other (see Fig. 1, *right*), it activates the second kinase by changing the structure of its activation loop. This allosteric mechanism, for which there is much experimental support, is described in detail elsewhere (6,12,13,15–17).

The available data suggest that the juxtamembrane domain (JMD), located between the transmembrane (TM) helix (*purple* in Fig. 1) and the structured kinase domain (*green* in Fig. 1), is natively unfolded or intrinsically disordered. It is conventionally shown as a flexible ''string'' in the cytoplasm (indicated by the *black wavy line* in Fig. 1). If the role of a ligand, such as EGF, is to cause the extracellular domains of two EGFR monomers to bind and thus bring together the intracellular kinase domains (as shown in Fig. 1, *right*), the flexible nature of the JMD extending into the cytoplasm is an asset. However, many experiments (18–23), including single-molecule (22,24) and fluorescence correlation spectroscopy measurements on living cells (25,26), strongly suggest that a fraction of the EGFR in the plasma membrane exists as preformed dimers, or oligomers (27–30) in the absence of a ligand. A fraction of the preformed dimers may comprise the high-affinity class of EGFRs (18,23,27), which appear to control the early response of the EGFR to EGF (31,32). This leads to an apparent paradox in terms of the model shown in Fig. 1. Why are the kinase domains of these preformed dimers not active in the absence of ligands? Specifically, if the JMD is flexible and free in the cytoplasm, why should the allosteric mechanism shown in the right-hand panel

Submitted December 1, 2008, and accepted for publication March 20, 2009.

Parijat Sengupta and Eran Bosis contributed equally to this work.

*Correspondence: Stuart.McLaughlin@stonybrook.edu

Editor: Lukas K. Tamm.

0006-3495/09/06/4887/9 $2.00

doi: 10.1016/j.bpj.2009.03.027

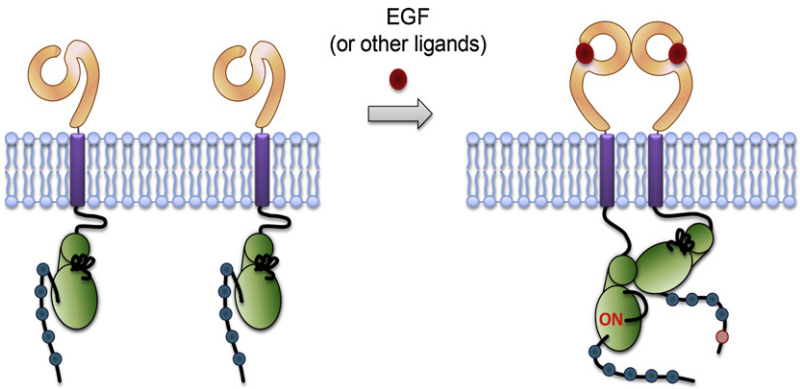

FIGURE 1 Cartoon of the dominant model for EGFR activation based on similar figures in previous studies (6,12,13,15). Binding of a ligand to the EGFR exposes a dimerization arm; lateral diffusion and binding of dimerization arms result in formation of a dimer. This allows the C-terminal or large lobe of one kinase domain to bind to the N-terminal lobe of the adjacent kinase domain and activate it by an allosteric mechanism (12). The activated kinase then phosphorylates tyrosine residues in the C-terminal tail region of the adjacent EGFR. The JMD is assumed to be free, flexible, and extended into the cytoplasm. An alternative ''twist'' model for activation (not shown) assumes that binding of EGF to each EGFR in a preformed dimer causes a rearrangement of the complex, perhaps a relative rotation of subunits (see text for discussion). The extracellular region of EGFR (*orange*), TM helix (*purple*), natively unfolded JMD (*black line*), kinase domain (*green*), and C-terminal tail (*black*) including tyrosine (*dark blue circles*) or phosphotyrosine (*orange*) residues are shown.

of Fig. 1 not always be operative for the preformed dimers? Perhaps there is an additional level of autoinhibition, other than the one exerted by the activation loop, that could explain why preformed dimers or oligomers are not always active. In other families of receptor tyrosine kinases, the JMD often exerts such an additional autoinhibitory role (11). We consider one specific autoinhibition mechanism in the Discussion section (see Fig. 5). We postulate that the positively charged JMD binds to the negatively charged inner leaflet, as does the positive face of the kinase domain (33–35). This prevents the two kinase domains from interacting, even if a significant fraction of EGFRs exist as preformed dimers or oligomers.

Our model allows the well-supported allosteric mechanism to be extended to the case of preformed dimers. In our model, the binding of EGF to the preformed dimer of EGFR produces two effects that contribute to activation. First, EGF reorganizes the preformed dimer (the implications of which are discussed below). Second, it produces a well-documented rapid increase in the cytoplasmic concentration of calcium ions, $[Ca^{2+}]_i$, which causes an increase in the local concentration of calcium/calmodulin (Ca/CaM). Calcium signaling is reviewed in detail elsewhere (36). The total concentration of calmodulin in a typical mammalian cell is in the range 20–50 μM (37,38). An increase in Ca/CaM allows it to bind to the JMD and reverse its charge from $+8$ to -8. This repels the Ca/CaM-JMD complex from the negatively charged inner leaflet of the plasma membrane; the adjacent kinase domain thus also moves off the membrane, contributing to activation (see Fig. 5). We provide pharmacological evidence elsewhere that Ca/CaM assists the process of trans-autophosphorylation of EGFR (35). Thus, it is of interest to understand the mechanism by which Ca/CaM competes with a membrane surface for the basic JMD of the EGFR, a known Ca/CaM-binding site in this receptor.

We envision two possible kinetic mechanisms by which Ca/CaM could enhance the fraction of time the JMD spends desorbed from the membrane, and thus enhance the activation of the EGFR. First, Ca/CaM could lurk in the cytoplasm, waiting for the JMD to spontaneously dissociate from the membrane, and then bind rapidly to it. Second, Ca/CaM could rip the membrane-bound JMD region from the plasma membrane, increasing the rate of JM domain dissociation from the surface. We performed experiments with fluorescently labeled peptides corresponding to the calmodulin-binding portion of the JMD, EGFR(645–660), and phospholipid vesicles of defined composition to distinguish between these two possibilities, at least for the model system.

The cytoplasmic leaflets of mammalian plasma membranes (39,40) contain 15–25% monovalent acidic lipids, mainly phosphatidylserine (PS), and 1–3% polyvalent acidic lipids, mainly phosphatidylinositol 4,5-bisphosphate (PIP_2). The EGFR JMD peptides bind with increasing avidity to phospholipid vesicles as the mole fractions of PS and PIP_2 are enhanced. In the Discussion section we extrapolate these measurements to the living cell and suggest that the binding of the JMD of the EGFR to the inner leaflet of the plasma membrane may be very strong in a quiescent cell. We speculate that Ca/CaM can only compete successfully with the membrane when ligand-induced reorganization of a preformed EGFR dimer forces two JMDs, each with a charge of $z = +8$, close together on the membrane surface. Close proximity of the JMDs both weakens their membrane binding and electrostatically attracts the negatively charged ($z = -16$) Ca/CaM.

MATERIALS AND METHODS

Materials

1-Palmitoyl-2-oleoyl-*sn*-glycero-3-phosphatidylcholine (PC), 1-palmitoyl-2-oleoyl-*sn*-glycero-3-phosphatidylserine (PS), 1-palmitoyl-2-oleoyl-*sn*-glycero-3- phosphatidyl-ethanolamine (PE), 1-oleoyl-2[12[7-nitro-2,1,3-benzoxadiazol-4-yl)amino]dodecanoyl]-*sn*-glycero-3-phospho-L-serine (NBD-PS), brain phosphatidylinositol 4,5-bisphosphate (PIP_2), and cholesterol were obtained from Avanti Polar Lipids (Alabaster, AL). Bovine brain calmodulin (phosphodiesterase 3′,5′-cyclic nucleotide-activator) was obtained from Sigma-Aldrich (St. Louis, MO). Acrylodan was purchased from Invitrogen (Carlsbad, CA).

The peptide acrylodan-EGFR(645–660) has the following sequence: acrylodan-CRRRHIVRKRTLRRLLQ. The acrylodan is attached covalently to the extra Cys residue added to the N-terminus of the peptide, which corresponds to the N-terminal, calmodulin-binding region of the JMD of the EGFR. The N- and C-terminal ends of the peptide are blocked with acetyl and amide groups, respectively. The peptide was obtained from American Peptide (Sunnyvale, CA). The acrylodan label was covalently attached to the Cys residue of the peptide at the NH_2 terminus (see Methods in the Supporting Material). The standard buffer solutions contained 100 mM KCl, 10 mM MOPS, pH = 7.0. Vesicle preparation and experiments were done at room temperature (22°C). Large unilamellar vesicles (LUVs) of diameters 100 and ~300 nm were prepared as described elsewhere (41).

Kinetic measurements

Fig. S1 illustrates the experimental protocol used to study the calmodulin-induced dissociation of acrylodan-EGFR(645–660) from vesicles, as documented in Figs. 2–4. As shown in Fig. 2 *A*, we measured the increase in fluorescence that occurred when the peptide moved from vesicles to calmodulin (excitation at 372 nm and emission at 466 nm). We designed the experiments so that most of the peptide was initially bound to the vesicles; after mixing with calcium/calmodulin (Ca/CaM), most of the peptide was bound to Ca/CaM.

RESULTS

The EGFR(645–660) peptide associates with LUVs with a rate constant, k_{on}, close to the diffusion-limited value

The kinetics of EGFR(645–660) association with membranes can be deduced by following the change in the fluorescence of an attached acrylodan probe. When acrylodan inserts into the low dielectric interior of the membrane, the fluorescence increases and is blue-shifted. As described in Section 1 of the Supporting Material, we determined the value of k_{on} by mixing acrylodan-labeled EGFR(645–660) and PC/PS vesicles and experimentally determining the relaxation time, τ, of their interaction. A plot of the reciprocal of the relaxation time ($1/\tau$) against vesicle concentration, [*V*], yields the forward rate constant, k_{on}:

$$1/\tau = k_{on}[V] + k_{off}. \quad (1)$$

We conclude for the EGFR(645–660) peptide, as for the other basic/unfolded peptides we have examined, that the forward rate constant does not differ significantly from the diffusion-limited value, k_{diff} (41,42). For 100 nm vesicles, this value is $k_{on} \sim k_{diff} = \sim 1 \times 10^{11}\ M^{-1}s^{-1}$. (As we discuss in Section 2 and Section 7 of the Supporting Material, the EGFR(645–660) peptide also associates with Ca/CaM with a rate constant close to the diffusion-limited value of $\sim 1 \times 10^{9}\ M^{-1}\ s^{-1}$, a result that is consistent with more detailed kinetic studies of the binding of Ca/CaM to other short peptides (43–45).

Ca/CaM increases the rate at which EGFR (645–660) dissociates from PC/PS membranes

Here we report kinetic measurements that address the question, Does Ca/CaM rip the JMD peptide off the membrane? Fig. S1 illustrates the experimental protocol.

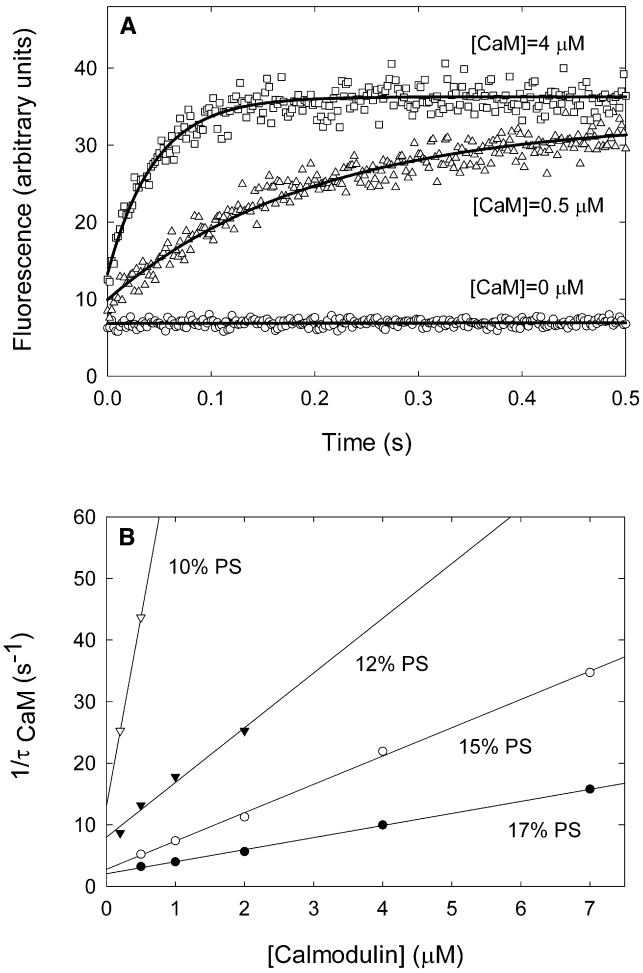

FIGURE 2 Ca/CaM enhances the rate of desorption of the EGFR JMD peptide from a PC/PS vesicle. (*A*) Kinetics of the transfer of acrylodan-EGFR(645–660) from PC/PS vesicles (15% PS) to Ca/CaM. Vesicles with membrane-bound peptide were mixed rapidly with a solution containing CaM to obtain a final Ca/CaM concentration in the mixing chamber of 0.5 μM (*triangles*) or 4 μM (*squares*). The experimental data points are the average of 10 shots. The curves are the single exponential fits to the data. Note that increasing [Ca/CaM] from 0.5 to 4 μM decreases the relaxation time constant ~4-fold. Additional experimental details are in the Methods section of the Supporting Material. (*B*) The reciprocal of the time constant ($1/\tau$) obtained from experiments shown in *A* and similar experiments is plotted versus [Ca/CaM] in the final mixing chamber. Note that both the intercept and slope increase as the mole fraction of PS in the vesicles decreases. The intercept is one measure of the spontaneous dissociation rate of the peptide from the vesicle; the slope is a measure of the transfer rate constant between the vesicle and Ca/CaM. The average values of these parameters are reported in Table 1.

The results shown in Fig. 2 *A* report measurements done on 100 nm diameter PC/PS LUVs with 15% PS. We chose conditions (e.g., lipid concentration) under which >90% of the peptide is bound initially to the vesicles. The vesicles contain 1% NBD-PS, which quenches the fluorescent probe acrylodan that is attached covalently to the N-terminal region of the peptide.

When the vesicles with membrane-bound peptide are mixed with a solution containing Ca/CaM (final [Ca/CaM] = 0.5 μM in the mixing chamber; *triangles* in Fig. 2 *A*), the peptide desorbs from the vesicles and binds to Ca/CaM, causing the fluorescence to increase ~4-fold. (Section 3 of the Supporting Material contains a discussion of the equilibrium affinity of the peptide for both membranes and Ca/CaM, and the effect of the acrylodan probe on these affinities.)

At a final [Ca/CaM] = 0.5 μM, the time constant (τ) for the movement of the peptide from vesicle to Ca/CaM is τ ~ 200 ms. The value of $1/\tau = 5\ s^{-1}$ is plotted in Fig. 2 *B* on the graph of $1/\tau$ vs. [Ca/CaM]. This value is not much faster than the spontaneous rate of dissociation of the peptide from the vesicle (obtained by extrapolation of the line in Fig. 2 *B* to [Ca/CaM] = 0, and by independent measurements discussed in Section 4 of the Supporting Material).

When the [Ca/CaM] in the mixing chamber is increased from 0.5 to 4 μM (*squares* in Fig. 2 *A*), the time constant for movement of the peptide from the vesicle to Ca/CaM decreases from 200 to ~45 ms. Equivalently, the rate at which the peptide moves off the membrane increases from $1/\tau = 5\ s^{-1}$ to $20\ s^{-1}$. This number is also plotted in Fig. 2 *B*. The ability of Ca/CaM to enhance the rate at which the peptide desorbs from the vesicles under our experimental conditions strongly suggests that Ca/CaM is ripping the peptide off the membrane in some manner, rather than just binding peptide that desorbs spontaneously with a fixed rate. A detailed analysis of the differential equations that describe the relaxation allows us to make this assertion (see Section 7 of the Supporting Material for a discussion of the expected results if Ca/CaM had not been able to rip the peptide from the surface).

Control measurements show that when vesicles with membrane-bound peptide are mixed with buffer solution that lacks either calcium ions or calmodulin (*circles* in Fig. 2 *A*), the peptide does not desorb significantly and the fluorescence does not increase.

The rate of dissociation of EGFR(645–660) from a vesicle is proportional to the [Ca/CaM]

Measurements similar to those in Fig. 2 *A* were repeated with different concentrations of Ca/CaM, and the results are plotted as open circles in Fig. 2 *B*. Note that the rate at which the peptide desorbs from the vesicle in the presence of Ca/CaM, $1/\tau_{CaM}$, is proportional to the [Ca/CaM]. The slope of the curve may be defined as the transfer rate constant, k_{trans}, which is $5 \times 10^6\ M^{-1}s^{-1}$ for the vesicles with 15% PS. The intercept of the line may be regarded as the spontaneous rate at which the peptide dissociates from the surface ($k_{off} = 3\ s^{-1}$ for this particular set of measurements). This result was averaged with the results of two other sets of independent measurements for 15% PS vesicles, and the average values of the intercept ($k_{off} = 5\ s^{-1}$) and slope ($k_{trans} = 6 \times 10^6\ M^{-1}s^{-1}$) are given in Table 1. The numbers are reported as the average ± SD for $n = 3$ sets of independent measurements.

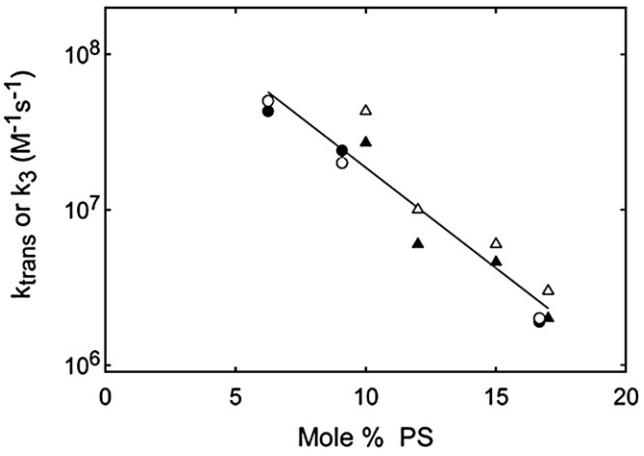

FIGURE 3 Transfer rate constant, k_{trans} (slope of the curves in Fig. 2 *B*), increases as the mole % PS in the membrane decreases. Data for EGFR(645–660) from Table 1 are shown as open triangles; data for MARCKS(151–175) peptide are shown as open circles. The rate constants for the interaction between Ca/CaM and the membrane-bound peptide, k_3 (see Section 7 of the Supporting Material), as calculated for EGFR(645–660) are shown as solid triangles; data for MARCKS(151–175) peptide are shown as solid circles.

The transfer rate constant increases 10-fold as the mole fraction of PS in the membrane decreases from 17% to 10%

Fig. 2 *B* shows that as the mole fraction of PS in the vesicles decreases, the transfer rate constant (slope) increases ~10-fold. This is shown more directly in Fig. 3, which plots the value of k_{trans} for the EGFR(645–660) peptide versus the mole fraction of PS in the vesicle. We define this process more precisely in Section 7 of the Supporting Material, where we present an analysis of the set of three coupled equations that describe the interaction of Ca/CaM, EGFR(645–660) and the membrane. The forward rate constant for the reaction between Ca/CaM and the membrane-bound peptide is defined as k_3 in Eq. S3. Fig. 3 shows that the transfer rate constant for EGFR(645–660), deduced from the slopes of lines in Fig. 2 *B*, is similar to the value of k_3, deduced from an analysis of the differential equations that describe the relaxation process, and their best fit to the kinetic data. Fig. 3 also shows that the transfer rate constant is identical, within experimental error, for a completely different peptide, MARCKS(151–175), that binds ~100-fold more strongly to Ca/CaM and a 5:1 PC/PS vesicle. A possible interpretation of this somewhat surprising result is discussed in Section 8 of the Supporting Material.

TABLE 1 Dissociation and transfer rate constants of EGFR(645–660) from PC/PS vesicles

% PS	k_{off} (s^{-1})	$k_{trans} \times 10^6$ ($M^{-1}s^{-1}$)
17	3 ± 2	3 ± 1
15	5 ± 2	6 ± 1
12	10 ± 5	10 ± 0.5
10	19 ± 5	43 ± 1.5

The spontaneous rate of dissociation of EGFR(645–660) from PC/PS vesicles also increases ~10-fold as the mole fraction of the acidic lipid PS decreases from 17% to 10%

We previously showed that the binding affinity (molar partition coefficient, K) of the EGFR(645–660) peptide to PC/PS vesicles increases exponentially with the mole fraction of monovalent acidic lipid (see Fig. S1 of McLaughlin et al. (33)). This is expected theoretically (46) and was observed experimentally with other basic and basic/hydrophobic peptides (e.g., see Rusu et al. (47)). Thus, if the forward rate constant, k_{on}, is diffusion-limited and independent of the binding affinity, increasing the mole fraction of PS, which increases $K = k_{on}/k_{off}$, should decrease k_{off}. All the data we have obtained are consistent with this prediction (see Table 1 and Section 4 of the Supporting Material).

The transfer rate constant is independent of the salt concentration

Fig. S9 shows that the transfer rate constant is independent of the salt concentration, at least in the range of 50–150 mM salt. In contrast, the molar partition coefficient K of the peptide onto the vesicles (the reciprocal of the lipid concentration required to bind 50% of the peptide) decreases markedly as the salt concentration is increased, as expected for electrostatic interactions (48,49). For example, K for the interaction of EGFR(645–660) with 2:1 PC/PS vesicles decreases 100-fold as the salt concentration increases from 100 to 200 mM (33). Thus, we anticipated that the rate constant for spontaneous movement of the peptide off the vesicle, $k_{off} = k_{on}/K$, would also increase as the salt concentration increases (because the diffusion-limited value of k_{on} should be independent of salt). Fig. S9 shows that k_{off} does increase as the salt concentration increases.

Incorporation of a physiological level of PIP_2 into PC/PS vesicles decreases the rate at which Ca/CaM can remove EGFR(645–660) from a vesicle

Fig. S4 shows that incorporating even a very low fraction of the multivalent acidic lipid PIP_2 into a PC/PS vesicle greatly decreases the rate at which Ca/CaM can rip the peptide from the membrane (i.e., incorporating 0.3% PIP_2 produces an order-of-magnitude decrease). The inner leaflet of a plasma membrane contains both monovalent acidic lipids, such as PS, and multivalent phosphoinositides, such as PIP_2, which typically comprises 1–3% of the phospholipids on the inner leaflet (50). Previous work showed that the membrane-adsorbed basic EGFR(645–660) peptide produces a local positive electrostatic potential that acts as a basin of attraction for multivalent phosphoinositides (51). The simple interpretation of the results shown in Fig. S4 is that PIP_2 is concentrated by nonspecific electrostatics adjacent to the membrane-adsorbed basic peptide, which greatly decreases the ability of Ca/CaM to rip the peptide off the surface.

Increasing the surface density of basic peptides adsorbed to a membrane to the point where the peptides repel each other increases both the spontaneous rate of desorption and the rate at which Ca/CaM can remove the EGFR(645–660) peptide

If binding of the JMD and kinase domain to the inner leaflet of the plasma membrane effectively inactivates the EGFR by preventing the two kinase domains from contacting each other (see Discussion for a figure that illustrates how this may occur), how does the allosteric activation mechanism proposed by Kuriyan and co-workers (12) ever function?

We consider here a corollary of the rotation model for activation of preformed dimers (19,52). Specifically, we assume that when two constituent EGFR monomers in a preformed dimer bind EGF and rotate, this brings together the membrane-bound JMD regions (e.g., Fig. 5). Simple electrostatic theory (53) indicates that pushing together the two +8 basic regions will cause one to spontaneously dissociate more rapidly from the membrane (k_{off} increases). Furthermore, the rate at which Ca/CaM can remove one basic JMD from the surface should also increase.

To study this phenomenon in a model system, we first enhanced the number of EGFR(645–660) peptides bound to a unit area of PC/PS membrane (i.e., increased the bound peptide/lipid ratio). When the peptides are closer on average than 2 Debye lengths ($1/\kappa$ ~1 nm) on the membrane, they repel each other electrostatically. We expected this repulsion to increase both the spontaneous rate of dissociation, k_{off}, and the rate at which Ca/CaM desorbs the peptide, k_{trans}, and that is what we observed (data not shown). However, the analysis is complicated because as Ca/CaM removes the peptide from the membrane, the surface coverage or number of peptides/area decreases, as does the phenomenon. To study the phenomenon under conditions in which the analysis is simpler, we added to the membrane extra basic clusters that are not removed by Ca/CaM. Specifically, we added a myristoylated peptide corresponding to the 18 N-terminal residues of Src (myristoylated-Src(2-19) = myr-Src peptide) to a PC/PS vesicle. The myr-Src peptide has a net charge of +5 (54). Control electrophoretic mobility measurements show that adding micromolar concentrations of the myr-Src peptide to the aqueous phase does allow the myr-Src peptide to bind to a degree that significantly reduces the net charge density of the PC/PS vesicles (17% PS) that we use for kinetic measurements. Specifically, the ζ-potential of a 5:1 PC/PS vesicle changes from -27 ± 1 mV to 0 mV upon addition of 1 μM myr-Src peptide, and to $+7 \pm 1$ mV upon addition of 3 μM myr-Src peptide. (The ζ-potential is proportional to the net charge/area on the membrane under our conditions.) Furthermore, Ca/CaM does not bind significantly to this myr-Src peptide under our conditions (adding Ca/CaM does not produce further changes in the ζ-potential). Thus, we can study how Ca/CaM pulls the

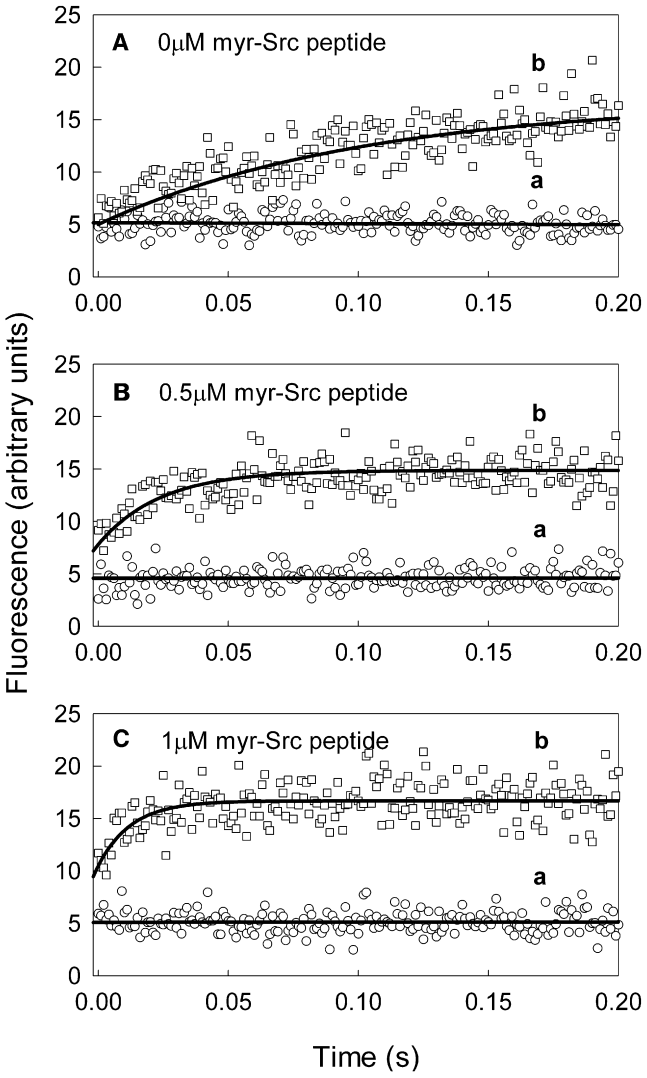

FIGURE 4 Binding of a myristoylated basic (net charge +5) peptide corresponding to the N-terminal 18-residue region of Src (myr-Src peptide) to a PC/PS phospholipid vesicle increases the rate at which Ca/CaM can dissociate the EGFR(645–660) peptide from the surface by 10-fold. Kinetics for the transfer of acrylodan-EGFR(645–660) from vesicles with 17% PS to 3 μM Ca/CaM, with 0 (*A*), 0.5 μM (*B*), and 1 μM (*C*) myr-Src peptide also present in the mixing chamber. The solid curves designated **b** show single exponential fits with the following relaxation times: (*A*) τ = 100 ms, (*B*) τ = 23 ms, and (*C*) τ = 13 ms. Additional experimental details are provided in the Methods section of the Supporting Material.

EGFR(645–660) peptide off the membrane when this peptide is adjacent to the myr-Src basic peptide (which is present at a high surface concentration of ~3 myr-Src peptides/100 lipids when the aqueous phase contains 1 μM peptide.). A molecular model of this myr-Src peptide adsorbed to a PC/PS bilayer is shown in Fig. 1 of Murray et al. (54). The results are shown in Fig. 4 for PC/PS membranes that contain 17% PS. The upper panel of Fig. 4 shows the results when the Myr-Src peptide is absent. Adding 3 μM Ca/CaM (final concentration in the mixing chamber) pulls the peptide off the PC/PS vesicle with a time constant of τ = 100 ms. Adding 0.5 μM (Fig. 4, *middle panel*) or 1 μM (Fig. 4, *bottom panel*) myr-Src peptide (final concentration in mixing chamber) decreased the time constants to ~20 and 10 ms, respectively. Thus, increasing the surface concentration of basic peptide can produce an order-of-magnitude increase in the rate at which Ca/CaM can pull the peptide off the surface. Put another way, Ca/CaM can compete more effectively with the membrane for the JMD when two basic regions are close together. The potential physiological implications of this result are discussed below.

DISCUSSION

Fig. 2 shows that Ca/CaM increases the rate of desorption of the EGFR(645–660) peptide from a phospholipid vesicle. The simplest interpretation is that Ca/CaM rips the peptide off the membrane. This interpretation is confirmed by a detailed analysis in Section 7 of the Supporting Material.

Ca/CaM is more effective at ripping the peptide off a surface for membranes with a lower mole fraction of acidic lipid. If the physiological mole fraction of PS is >20%, however, Ca/CaM barely increases the spontaneous rate of dissociation (Fig. 2 *B*), and addition of PIP_2 further decreases the rate (Fig. S4 and Fig. S5).

Equilibrium measurements with simple JMD peptides (33) and reconstituted peptides corresponding to the TM + JMD regions of EGFR (34) are in accord with the kinetic data reported here with EGFR(645–660) peptides adsorbed to phospholipid vesicles. If we extrapolate these results to the biological membrane, they suggest that the JMD of the EGFR binds sufficiently strongly to the inner leaflet that it rarely comes off the negatively charged membrane. Furthermore, even when the level of Ca/CaM increases to the maximum physiological value (~10 μM), the available kinetic and equilibrium data suggest that it cannot compete with the strong electrostatic binding of an *isolated* JMD to the membrane.

If the binding is so strong that the JMD (and attached kinase domain) rarely come off the membrane, how is activation of the EGFR achieved? The results reported in Fig. 4 provide one clue. If two JMD peptides come close together (or one comes close to another membrane-adsorbed basic cluster, such as on the myr-Src peptide), both the spontaneous rate of desorption and the rate at which Ca/CaM can remove the JMD peptide are greatly enhanced, as expected from simple electrostatic considerations. We suggest that a similar phenomenon may occur with EGFR in a living cell.

Model of EGFR activation

Our view of the structure of a single EGFR molecule in the plasma membrane is shown in Fig. 5 *A*. The structural domains of the EGFR are shown to scale. The figure

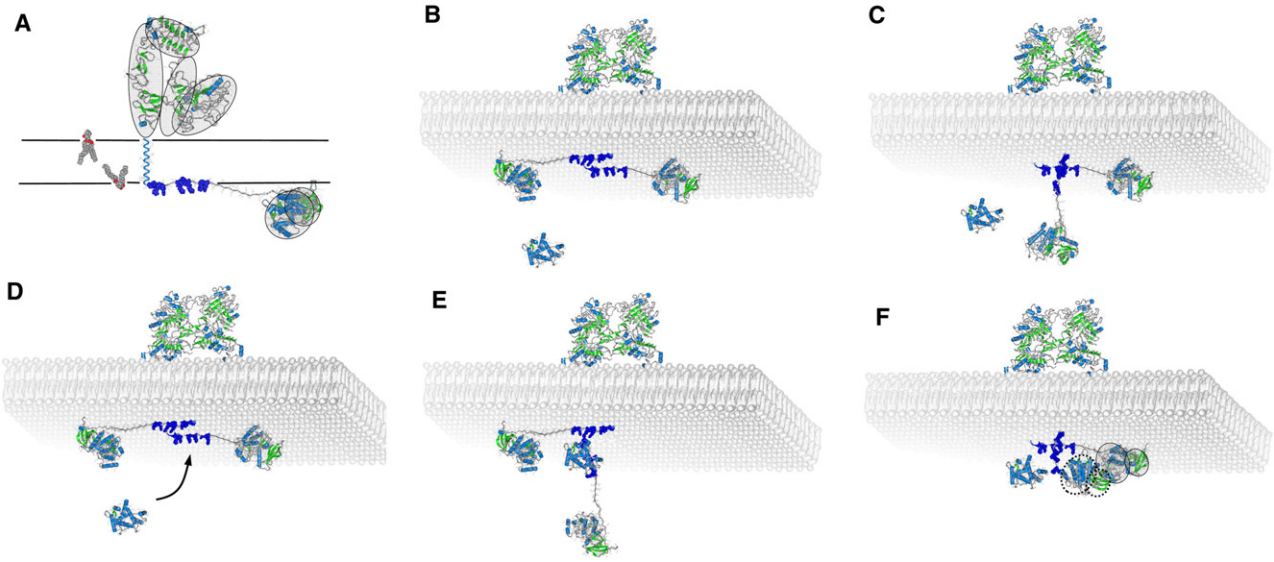

FIGURE 5 Proposed mechanism of activation of EGFR. (*A*) Proposed structure of an EGFR monomer in a quiescent cell. The extracellular domain has the structure determined from x-ray analysis, as reviewed by Ferguson (6). The N-terminal portion of the intracellular JMD (residues 645–660 of the JMD), with the eight basic residues shown in blue, is postulated to bind electrostatically to the inner leaflet of the plasma membrane. The basic face of the kinase domain (see Fig. 2 of McLaughlin et al. (33)) for the electrostatic potential profile) is also postulated to bind to the negatively charged inner leaflet of the plasma membrane, but less strongly than the JMD. For simplicity, the C-terminal tail of the EGFR is not shown. (*B*) View from the cytoplasm. Two monomers form a dimer (of known extracellular structure) upon binding of EGF. Alternatively, binding of EGF mediates rotation of the subunits of a preformed dimer to the same extracellular structure. We hypothesize that in either case the intracellular basic JM regions come into proximity. Calmodulin is shown in the cytoplasm. (*C*) The electrostatic repulsion between the two highly charged JMDs weakens their attraction to the membrane. This causes one of the JMDs and its associated kinase domain to dissociate. (*D*) Alternatively, and in addition to the spontaneous dissociation shown in panel *C*, Ca/CaM binds to one of the JMD and rips it from the membrane, resulting in the conformation shown in panel *E*. The proximity of the second JMD greatly facilitates this process. Our measurements are consistent with the hypothesis that Ca/CaM can only compete with the membrane for binding of the JM region when the two JMDs are close together as in panel *B*. (*E*) Ca/CaM binding to the JMD of one of the EGFR molecules in a dimer causes it and the associated kinase region to dissociate from the membrane. Activation of the kinase domain by an allosteric mechanism (12) can proceed from the conformations shown in either panel *E* or *C*. In panel *F*, we assume activation proceeds from the conformation shown in panel *C*. (*F*) The N-terminal lobe (small lobe, colored *green*) binds to the C-terminal lobe of the membrane-bound kinase domain and is activated by an allosteric mechanism (12).

illustrates two key postulates concerning the positively charged JMD that emerge from our measurements.

First, we postulate that both the positively charged JMD and the positive face of the kinase domain are bound to the inner leaflet of the plasma membrane. We assume this is true for both monomeric EGFR and for both of the two EGFR molecules in a preformed dimer that exists in the absence of ligand. There is evidence from many different laboratories that preformed dimers of EGFR exist in the absence of ligands (18–23,25,26). There is also evidence from cleverly designed molecular biology experiments that binding of EGF causes rotation of the constituents of a preformed EGFR dimer (19,52), and we suggest that this may cause the two JM regions to come together as shown in Fig. 5 *B*. (Alternatively, if two monomers are joined together by the dimerization arms after two EGF ligands bind, or two preformed dimers come together to form a tetramer (27), the membrane-bound JMD could be positioned close together as shown in Fig. 5 *B*).

Second, we postulate that if the two JMDs come within 2 Debye lengths of each other (Debye length $= 1/\kappa \sim 1$ nm in physiological salt), they will significantly repel each other and thus weaken their net interaction with the membrane. The spontaneous rate of desorption from the membrane, k_{off}, will increase. This is shown in Fig. 5 *C*, which indicates that one JMD + kinase domain has desorbed from the surface spontaneously. In addition, when the $[Ca^{2+}]_i$ and thus the concentration of Ca/CaM increases (which happens rapidly after binding of EGF to the EGFR), Ca/CaM can bind to one of the two adjacent membrane-bound JMD, as shown by the arrow in Fig. 5 *D*, causing it to desorb more rapidly, as shown in Fig. 5 *E*. Activation of a kinase domain by the allosteric mechanism could proceed from either the situation in Fig. 5 *C* (one JMD + kinase domain spontaneously desorbed) or Fig. 5 *E* (one JMD dissociated by Ca/CaM and accompanied by the kinase domain moving off the membrane). Fig. 5 *F* shows the activation process that occurs after the spontaneous desorption shown in Fig. 5 *C*. In Fig. 5 *F*, the C-terminal lobe of the membrane-bound kinase domain is binding to and activating the N-terminal lobe of the cytoplasmic kinase domain by the allosteric mechanism described previously (12,55). Ca/CaM is shown adjacent to the kinase domain to illustrate its relative size. When bound to the JMD, as in Fig. 5 *E*, Ca/CaM could stabilize the activation of the kinase by the allosteric mechanism shown in Fig. 5 *F*.

This mechanism is speculative. However, it is specific and has a number of corollaries that can be tested.

For example, increasing the ionic strength of the cytoplasm weakens the electrostatic interaction of the JMD (and kinase domain) for the membrane (33). The strong effect of salt in decreasing the electrostatic interaction of clusters of basic residues with membranes is well understood from the first principles of physics (48). Thus, we would expect an increase in the ionic strength of the cytoplasm to activate the EGFR in the absence of ligand; it does (56,57).

Furthermore, making the inner leaflet of the plasma membrane less negatively charged by the addition of amphipathic weak bases, such as sphingosine, to the bathing solution should activate the EGFR in the absence of ligands. This should occur at the aqueous concentration of the weak base (e.g., sphingosine) that reverses the net charge of a bilayer (~2 μM); it does (58). Furthermore, all amphipathic weak bases should have this effect. We have tested this prediction for several weak bases and confirmed the prediction for all the chemicals we investigated (35). In Section 10 of the Supporting Material we discuss three other predictions of the model shown in Fig. 5.

We note that there are three simple biophysical concepts or ''cheap tricks'' (59) involved in the activation of the EGFR in the model illustrated in Fig. 5: reduction of dimensionality, electrostatics, and coincidence counting. Reduction of dimensionality is important because the JMD is anchored to the membrane surface by the TM region and experiences a 1000-fold higher local concentration of lipid than if it were dissolved in the cytoplasm (60). Electrostatics is important because it produces the main energy that anchors the JMD and kinase domain to the membrane. Finally, full activation of the EGFR in our model is observed only when two phenomena occur together: 1), a ligand binds to the extracellular region and brings the two basic JMD together on the surface (Fig. 5 *B*); and 2), the level of Ca/CaM rises in the cell, ripping the JMD off the membrane (Fig. 5, *D* and *E*) and enhancing the time a kinase domain spends off the membrane.

In addition to these biophysical cheap tricks, there are two well-established major elements of the activation mechanism involved in the model presented in Fig. 5: 1), the mechanism by which EGF releases the tethered state (6) and allows dimer formation or rearrangement within a preformed dimer; and 2), the allosteric activation mechanism of the kinase domain (12). These aspects of the overall activation mechanism seem likely to be retained in any future model.

SUPPORTING MATERIAL

Methods, results, discussion, figures, a table, and references are available at http://www.biophysj.org/biophysj/supplemental/S0006-3495(09)00769-3.

This work was supported by grants from the National Institutes of Health to S.McL. (GM 24971) and S.S. (GM 46732).

REFERENCES

1. Carpenter, G. 2000. The EGF receptor: a nexus for trafficking and signaling. *Bioessays*. 22:697–707.
2. Schlessinger, J. 2000. Cell signaling by receptor tyrosine kinases. *Cell*. 103:211–225.
3. Yarden, Y., and M. X. Sliwkowski. 2001. Untangling the ErbB signalling network. *Nat. Rev. Mol. Cell Biol*. 2:127–137.
4. Jorissen, R. N., F. Walker, N. Pouliot, T. P. J. Garrett, C. W. Ward, et al. 2003. Epidermal growth factor receptor: mechanisms of activation and signalling. *Exp. Cell Res*. 284:31–53.
5. Citri, A., and Y. Yarden. 2006. EGF-ErbB signalling: towards the systems level. *Nat. Rev. Mol. Cell Biol*. 7:505–516.
6. Ferguson, K. M. 2008. Structure-based view of epidermal growth factor receptor regulation. *Annu. Rev. Biophys*. 37:353–373.
7. Blume-Jensen, P., and T. Hunter. 2001. Oncogenic kinase signalling. *Nature*. 411:355–365.
8. Holbro, T., G. Civenni, and N. E. Hynes. 2003. The ErbB receptors and their role in cancer progression. *Exp. Cell Res*. 284:99–110.
9. Landau, M., and N. Ben-Tal. 2008. Dynamic equilibrium between multiple active and inactive conformations explains regulation and oncogenic mutations in ErbB receptors. *Biochim. Biophys. Acta*. 1785:12–31.
10. Kong, A., V. R. Calleja, P. Leboucher, A. Harris, P. J. Parker, et al. 2008. HER2 oncogenic function escapes EGFR tyrosine kinase inhibitors via activation of alternative HER receptors in breast cancer cells. *PLoS ONE*. 3:e2881.
11. Hubbard, S. R. 2004. Juxtamembrane autoinhibition in receptor tyrosine kinases. *Nat. Rev. Mol. Cell Biol*. 5:464–471.
12. Zhang, X., J. Gureasko, K. Shen, P. A. Cole, and J. Kuriyan. 2006. An allosteric mechanism for activation of the kinase domain of epidermal growth factor receptor. *Cell*. 125:1137–1149.
13. Ward, C. W., M. C. Lawrence, V. A. Streltsov, T. E. Adams, and N. M. McKern. 2007. The insulin and EGF receptor structures: new insights into ligand-induced receptor activation. *Trends Biochem. Sci*. 32:129–137.
14. Burgess, A. W., H.-S. Cho, C. Eigenbrot, K. M. Ferguson, T. P. J. Garrett, et al. 2003. An open-and-shut case? Recent insights into the activation of EGF/ErbB receptors. *Mol. Cell*. 12:541–552.
15. Hubbard, S. R. 2006. EGF receptor activation: push comes to shove. *Cell*. 125:1029–1031.
16. Hubbard, S. R., and W. T. Miller. 2007. Receptor tyrosine kinases: mechanisms of activation and signaling. *Curr. Opin. Cell Biol*. 19:117–123.
17. Qiu, C., M. K. Tarrant, S. H. Choi, A. Sathyamurthy, R. Bose, et al. 2008. Mechanism of activation and inhibition of the HER4/ErbB4 kinase. *Structure*. 16:460–467.
18. Gadella, Jr., T., and T. Jovin. 1995. Oligomerization of epidermal growth factor receptors on A431 cells studied by time-resolved fluorescence imaging microscopy. A stereochemical model for tyrosine kinase receptor activation. *J. Cell Biol*. 129:1543–1558.
19. Moriki, T., H. Maruyama, and I. N. Maruyama. 2001. Activation of preformed EGF receptor dimers by ligand-induced rotation of the transmembrane domain. *J. Mol. Biol*. 311:1011–1026.
20. Martin-Fernandez, M., D. T. Clarke, M. J. Tobin, S. V. Jones, and G. R. Jones. 2002. Preformed oligomeric epidermal growth factor receptors undergo an ectodomain structure change during signaling. *Biophys. J*. 82:2415–2427.
21. Yu, X., K. D. Sharma, T. Takahashi, R. Iwamoto, and E. Mekada. 2002. Ligand-independent dimer formation of epidermal growth factor receptor (EGFR) is a step separable from ligand-induced EGFR signaling. *Mol. Biol. Cell*. 13:2547–2557.
22. Teramura, Y., J. Ichinose, T. Hiroaki, K. Nishida, T. Yanagida, et al. 2006. Single-molecule analysis of epidermal growth factor binding on the surface of living cells. *EMBO J*. 25:4215–4222.

23. Webb, S. E. D., S. K. Roberts, S. R. Needham, C. J. Tynan, D. J. Rolfe, et al. 2008. Single-molecule imaging and fluorescence lifetime imaging microscopy show different structures for high- and low-affinity epidermal growth factor receptors in A431 cells. *Biophys. J.* 94:803–819.
24. Sako, Y., S. Minoghchi, and T. Yanagida. 2000. Single-molecule imaging of EGFR signalling on the surface of living cells. *Nat. Cell Biol.* 2:168–172.
25. Liu, P., T. Sudhaharan, R. M. L. Koh, L. C. Hwang, S. Ahmed, et al. 2007. Investigation of the dimerization of proteins from the epidermal growth factor receptor family by single wavelength fluorescence cross-correlation spectroscopy. *Biophys. J.* 93:684–698.
26. Saffarian, S., Y. Li, E. L. Elson, and L. J. Pike. 2007. Oligomerization of the EGF receptor investigated by live cell fluorescence intensity distribution analysis. *Biophys. J.* 93:1021–1031.
27. Clayton, A. H. A., F. Walker, S. G. Orchard, C. Henderson, D. Fuchs, et al. 2005. Ligand-induced dimer-tetramer transition during the activation of the cell surface epidermal growth factor receptor-A multidimensional microscopy analysis. *J. Biol. Chem.* 280:30392–30399.
28. Clayton, A. H. A., M. L. Tavarnesi, and T. G. Johns. 2007. Unligated epidermal growth factor receptor forms higher order oligomers within microclusters on A431 cells that are sensitive to tyrosine kinase inhibitor binding. *Biochemistry.* 46:4589–4597.
29. Clayton, A. H. A., S. G. Orchard, E. C. Nice, R. G. Posner, and A. W. Burgess. 2008. Predominance of activated EGFR higher-order oligomers on the cell surface. *Growth Factors.* 26:316–324.
30. Whitson, K. B., J. M. Beechem, A. H. Beth, and J. V. Staros. 2004. Preparation and characterization of Alexa Fluor 594-labeled epidermal growth factor for fluorescence resonance energy transfer studies: application to the epidermal growth factor receptor. *Anal. Biochem.* 324:227–236.
31. Defize, L., J. Boonstra, J. Meisenhelder, W. Kruijer, L. Tertoolen, et al. 1989. Signal transduction by epidermal growth factor occurs through the subclass of high affinity receptors. *J. Cell Biol.* 109:2495–2507.
32. Bellot, F., W. Moolenaar, R. Kris, B. Mirakhur, I. Verlaan, et al. 1990. High-affinity epidermal growth factor binding is specifically reduced by a monoclonal antibody, and appears necessary for early responses. *J. Cell Biol.* 110:491–502.
33. McLaughlin, S., S. O. Smith, M. J. Hayman, and D. Murray. 2005. An electrostatic engine model for autoinhibition and activation of the epidermal growth factor receptor (EGFR/ErbB) family. *J. Gen. Physiol.* 126:41–53.
34. Sato, T., P. Pallavi, U. Golebiewska, S. McLaughlin, and S. O. Smith. 2006. Structure of the membrane reconstituted transmembrane-juxtamembrane peptide EGFR(622–660) and its interaction with Ca^{2+}/calmodulin. *Biochemistry.* 45:12704–12714.
35. Sengupta, P., M. J. Ruano, F. Tebar, U. Golebiewska, I. Zaitseva, et al. 2007. Membrane-permeable calmodulin inhibitors (e.g. W-7/W-13) bind to membranes, changing the electrostatic surface potential: dual effect of W-13 on epidermal growth factor receptor activation. *J. Biol. Chem.* 282:8474–8486.
36. Clapham, D. E. 2007. Calcium signaling. *Cell.* 131:1047–1058.
37. Black, D. J., Q.-K. Tran, and A. Persechini. 2004. Monitoring the total available calmodulin concentration in intact cells over the physiological range in free Ca^{2+}. *Cell Calcium.* 35:415–425.
38. Tran, Q.-K., D. J. Black, and A. Persechini. 2005. Dominant affectors in the calmodulin network shape the time courses of target responses in the cell. *Cell Calcium.* 37:541–553.
39. Holthuis, J. C. M., and T. P. Levine. 2005. Lipid traffic: floppy drives and a superhighway. *Nat. Rev. Mol. Cell Biol.* 6:209–220.
40. van Meer, G., D. R. Voelker, and G. W. Feigenson. 2008. Membrane lipids: where they are and how they behave. *Nat. Rev. Mol. Cell Biol.* 9:112–124.
41. Arbuzova, A., J. Wang, D. Murray, J. Jacob, D. S. Cafiso, et al. 1997. Kinetics of interaction of the myristoylated alanine-rich C kinase substrate, membranes, and calmodulin. *J. Biol. Chem.* 272:27167–27177.
42. Arbuzova, A., D. Murray, and S. McLaughlin. 1998. MARCKS, membranes, and calmodulin: kinetics of their interaction. *Biochim. Biophys. Acta.* 1376:369–379.
43. Torok, K., and D. R. Trentham. 1994. Mechanism of 2-chloro-(ε-amino-Lys_{75}) - [6-[4-(N,N-diethylamino)phenyl]-1,3,5-triazin-4-yl]-calmodulin interactions with smooth muscle myosin light chain kinase and derived peptides. *Biochemistry.* 33:12807–12820.
44. Brown, S. E., S. R. Martin, and P. M. Bayley. 1997. Kinetic control of the dissociation pathway of calmodulin-peptide complexes. *J. Biol. Chem.* 272:3389–3397.
45. Torok, K. 2002. Calmodulin conformational changes in the activation of protein kinases. *Biochem. Soc. Trans.* 30:55–61.
46. Arbuzova, A., L. Wang, J. Wang, G. Hangyas-Mihalyne, D. Murray, et al. 2000. Membrane binding of peptides containing both basic and aromatic residues. Experimental studies with peptides corresponding to the scaffolding region of caveolin and the effector region of MARCKS. *Biochemistry.* 39:10330–10339.
47. Rusu, L., A. Gambhir, S. McLaughlin, and J. Radler. 2004. Fluorescence correlation spectroscopy studies of peptide and protein binding to phospholipid vesicles. *Biophys. J.* 87:1044–1053.
48. Ben-Tal, N., B. Honig, R. M. Peitzsch, G. Denisov, and S. McLaughlin. 1996. Binding of small basic peptides to membranes containing acidic lipids: theoretical models and experimental results. *Biophys. J.* 71:561–575.
49. Ben-Tal, N., B. Honig, C. Miller, and S. McLaughlin. 1997. Electrostatic binding of proteins to membranes. Theoretical predictions and experimental results with charybdotoxin and phospholipid vesicles. *Biophys. J.* 73:1717–1727.
50. Golebiewska, U., M. Nyako, W. Woturski, I. Zaitseva, and S. McLaughlin. 2008. Diffusion coefficient of fluorescent phosphatidylinositol 4,5-bisphosphate in the plasma membrane of cells. *Mol. Biol. Cell.* 19:1663–1669.
51. McLaughlin, S., and D. Murray. 2005. Plasma membrane phosphoinositide organization by protein electrostatics. *Nature.* 438:605–611.
52. Bell, C. A., J. A. Tynan, K. C. Hart, A. N. Meyer, S. C. Robertson, et al. 2000. Rotational coupling of the transmembrane and kinase domains of the neu receptor tyrosine kinase. *Mol. Biol. Cell.* 11:3589–3599.
53. Murray, D., A. Arbuzova, G. Hangyas-Mihalyne, A. Gambhir, N. Ben-Tal, et al. 1999. Electrostatic properties of membranes containing acidic lipids and adsorbed basic peptides: theory and experiment. *Biophys. J.* 77:3176–3188.
54. Murray, D., L. Hermida-Matsumoto, C. A. Buser, J. Tsang, C. T. Sigal, et al. 1998. Electrostatics and the membrane association of Src: theory and experiment. *Biochemistry.* 37:2145–2159.
55. Pellicena, P., and J. Kuriyan. 2006. Protein-protein interactions in the allosteric regulation of protein kinases. *Curr. Opin. Struct. Biol.* 16:702–709.
56. King, C. R., I. Borrello, L. Porter, P. Comoglio, and J. Schlessinger. 1989. Ligand-independent tyrosine phosphorylation of EGF receptor and the erbB-2/neu proto-oncogene product is induced by hyperosmotic shock. *Oncogene.* 4:13–18.
57. Rodríguez, I., M. Kaszkin, A. Holloschi, K. Kabsch, M. M. Marqués, et al. 2002. Hyperosmotic stress induces phosphorylation of cytosolic phospholipase A2 in HaCaT cells by an epidermal growth factor receptor-mediated process. *Cell. Signal.* 14:839–848.
58. Davis, R., N. Girones, and M. Faucher. 1988. Two alternative mechanisms control the interconversion of functional states of the epidermal growth factor receptor. *J. Biol. Chem.* 263:5373–5379.
59. McLaughlin, S., J. Wang, A. Gambhir, and D. Murray. 2002. PIP_2 and proteins: interactions, organization, and information flow. *Annu. Rev. Biophys. Biomol. Struct.* 31:151–175.
60. Kuriyan, J., and D. Eisenberg. 2007. The origin of protein interactions and allostery in colocalization. *Nature.* 450:983–990.